International Journal of Advanced Engineering Research and Science (IJAERS)
Peer-Reviewed Journal
ISSN: 2349-6495(P) | 2456-1908(O)
Vol-9, Issue-12; Dec, 2022
Journal Home Page Available: https://ijaers.com/
Article DOI: https://dx.doi.org/10.22161/ijaers.912.46

# Anomaly Detection Applied to ISHM for Thickness Reduction Analysis in Controlled Environments

Alexsander L. Lima[1], Stanley W. F. Rezende[2], Diogo S. Rabelo[3], Quintiliano S. S. Nomelini[4], José Waldemar Silva[4], Roberto M. Finzi Neto[2], Carlos A. Gallo[2], José dos Reis V. Moura Jr[1]

[1]Mathematics and Technology Institute (IMTEC), Federal University of Catalao (UFCAT), Brazil
[2]Faculty of Mechanical Engineering, Federal University of Uberlandia (UFU), Uberlandia, Brazil
[3]Faculty of Sciences and Technology, Federal University of Goias (UFG), Aparecida de Goiania, Brazil
[4]Faculty of Mathematics (FAMAT), Federal University of Uberlandia (UFU), Uberlandia, Brazil

Received: 24 Nov 2022,
Receive in revised form: 17 Dec 2022,
Accepted: 23 Dec 2022,
Available online: 31 Dec 2022



***Keywords*— Anomaly analysis, Machine learning, Structural health monitoring.**

***Abstract*** *— In this work, three machine learning approaches were evaluated for detecting anomalies in impedance-based structural health monitoring (ISHM – Impedance-based Structural Health Monitoring) of a specimen in a controlled environment. Supervised, unsupervised, and semi-supervised algorithms were chosen to compare them regarding detecting anomalies in an aluminum beam with failure induced by surface machining on one of the faces. After applying the algorithms, it was found that, of the three types of learning, supervised and semi-supervised were the ones that achieved the best accuracy in detecting anomalies. On the other hand, the unsupervised type model did not obtain good results for the conditions investigated. Thus, this can be an important technique comparison achievement for implementing real anomaly detection ISHM systems.*

## I. INTRODUCTION

In the last decades, with the constant evolution of several technologies, it has been possible to build several highly complex machines and structures. With these advances, some actions are necessary to guarantee the proper functioning of the equipment or a stable construction of some structure, such as, for example, more prepared workers/operators, raw material with better quality and more complex maintenance, and failures that generally can generate significant financial losses or in more severe cases, loss of life [8].

In corrective maintenance, the repair of the structure is done immediately, implying the stoppage of the same to carry out the maintenance. This type of maintenance corresponds to a reaction to events that have occurred. Therefore, in the event of an unforeseen anomaly, the production of a machine or the use of a particular structure is stopped immediately, which can lead to a significant loss of time, high financial losses, and, depending on the severity of the defect, loss of life [9].

One of the several methods used in predictive maintenance is Structural Health Monitoring based on Electromechanical Impedance – ISHM. This technique aims to identify the properties of the structure about the occurrence of anomalies. Using the direct and inverse properties of certain piezoelectric materials, the method consists of fixing a sensor in the form of a PZT patch (Lead Zirconate Titanate) in the structure, which, after being excited at high frequency, around of 30kHz, causes the structure to undergo deformation, which consequently causes vibrations in the structure [3].

On the other hand, numerous machine learning techniques have been constantly developed to solve increasingly complex problems. As an example, there are anomaly

detection models that, with recent technological advances, have significantly impacted the maintenance sector [11].

In this way, the purpose of this work is to use anomaly analysis models based on supervised, unsupervised, and semi-supervised machine learning methods, with data collected from the monitoring of the structural integrity made in an aluminum beam to identify faults that were imposed on the surface of the specimen.

## II. METHODOLOGY

Piezoelectric materials are widely used in the implementation of SHM due to their direct and inverse properties, the best known being Lead Zirconate Titanate (PZT - Pb-Lead Zirconate Titanate). In the inverse effect, changes occur in its dimensions concerning the application of the electrical potential difference, expressed by equation (1), and this phenomenon is used as an actuator [10] [7].

$$D = \varepsilon E + d\sigma, \tag{1}$$

where, $D$ is the strain vector, $\varepsilon$ is the dielectric tensor of the material, $E$ is the electric field vector, $d$ is the piezoelectric voltage tensor, and $\sigma$ is the voltage vector [10] [7].

In the direct effect, changes in electrical properties occur due to mechanical deformations, expressed by equation (2), functioning as a sensor [10] [7].

$$e = s\sigma + dE, \tag{2}$$

where *e* is the strain tensor, and *s* is the elastic property of the piezoelectric material [10] [7].

In 1994, Liang, Sun, and Rogers published a work where a model capable of identifying the process of measuring electromechanical impedance for one degree of freedom was presented. Combining the functions of the mechanical impedance of the PZT patch, $Z_a$ and the mechanical impedance of the structure *Z*, the admittance function *Y* (inverse of impedance) is created, shown in equation (3) [5].

$$Y = i\omega \frac{w_a l_a}{h_a}\left(\overline{\varepsilon_{33}^{T}} - \frac{Z}{Z_a - Z} d_{32}^2 \overline{Y}_{22}^{E}\right), \tag{3}$$

where, $i$ is the output current of the PZT wafer, ω is the angular frequency, $w_a$ is the width of the PZT wafer, $l_a$ is the length of the PZT wafer, $h_a$ is the thickness of the PZT wafer, $\overline{\varepsilon}_{33}^{T}$ is the complex dielectric constant of the PZT wafer at zero voltage, $d_{32}^2$ is the piezoelectric constant and $\overline{Y}_{22}^{E}$ is Young's complex modulus of the PZT wafer with zero electric fields [5].

With the piezoelectric sensor/actuator fixed in the structure, the monitoring measures the real part of the impedance signature (IS). Then, a comparison is made between the signatures of the structure in its natural state with the signatures resulting from damage to locate/measure the level of the problem. This comparison can be made using the damage metric, Root Mean Square Deviation (RMSD), shown by equation (4), or if it is necessary to grant a specific value about the distinction between two sets, the Coefficient Deviation index (CCD - Correlation Coefficient Deviation), shown by equation (5) [3].

$$RMSD = \sqrt{\frac{\sum[\mathrm{Re}(Z) - \mathrm{Re}(Z^0)]^2}{\sum[\mathrm{Re}(Z^0)]^2}}, \tag{4}$$

where $\mathrm{Re}(Z)$ represents the real part of the PZT measured under healthy conditions and $\mathrm{Re}(Z^0)$ represents the real part of the signal to be compared [3].

$$CCD = 1 - CC, \tag{5}$$

CC is the correlation coefficient calculated using equation (6) [3].

$$CC = \frac{1}{\sigma_Z \sigma_{Z^0}} \sum[\mathrm{Re}(Z) - \mathrm{Re}(\overline{Z})][\mathrm{Re}(Z^0) - \mathrm{Re}(\overline{Z}^0)], \tag{6}$$

where $\sigma_Z$ is the standard deviation of the impedance signal measured under healthy conditions, $\sigma_{Z^0}$ is the standard deviation of the impedance signal to be compared, $\overline{Z}$ and $\overline{Z}^0$ represent the mean values [3].

There are several machine learning techniques, which can be classified depending on specific attributions such as being trained with supervision (labels) or not; by the grouping of peers; whether they can learn quickly; whether they can compare known data points with new data points, and whether they detect patterns to create predictive models. There is no exclusivity in using these techniques; merging more than one technique is possible to arrive at the best solution [2].

As mentioned in Section 1, anomaly detection models based on supervised, unsupervised and semi-supervised machine learning techniques will be used, using the algorithms: Logistic Regression, Copula-based Anomaly Detection (COPOD - Copula- Based Outlier Detection), and Local Outlier Factor (LOF).

Starting with the supervised type model, the Logistic Regression algorithm aims to separate two classes, the

inliers (non-atypical data) and outliers (atypical data) sets. Using this technique, it is possible to make the relationship between the dependent variables, also known as labels (y), such as (0 or 1), with the independent variables (X) [6]. Equation (7) represents logistic regression.

$$P(y=1)=\frac{1}{1+e^{-(B_0+B_1X_1+B_nX_n)}}, \quad (7)$$

where, *X* represents the independent variables (model inputs) and *B* are estimated by the maximum likelihood method, which aims to maximize the probability that the data set has been observed [6].

Varying the values of *X*, it is possible to observe that the curve behaves in the shape of the letter "S", shown in Fig. 1, reaching a high degree of generalization [6].

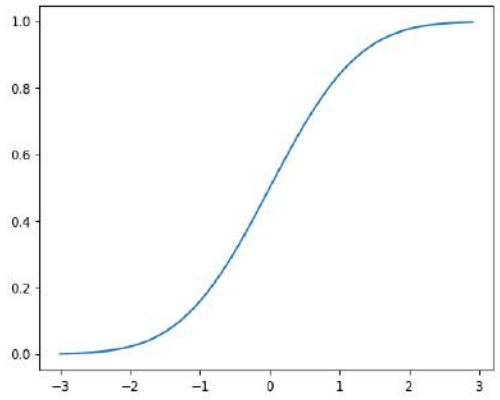


*Fig. 1: Logistic Regression Curve.*

For the development of an unsupervised model, the COPOD algorithm was used, which is based on empirical cumulative distribution functions (ECDFs), whose format is given according to equation (8) [4].

$$F(x)=P((-\infty,x])=\frac{1}{n}\sum_{i=1}^{n}(X_i\leq x), \quad (8)$$

Where *X* is a d-dimensional dataset and *n* is the number of observations. This algorithm is based on copulas, which are functions to separate distributions of systems dependent on a multivariate arrangement, shown by equation (9) [4].

$$C_u(u)=P(U_1\leq u_1,...,U_d\leq u_d), \quad (9)$$

where, *U* is a random vector and $u \in [0, 1]$. Since this algorithm is deterministic, there is no need to create hyperparameters (parameters to be defined before training). Therefore, problems with possible biases can be avoided. Regarding efficiency, the COPOD algorithm is one of the leading choices when the sample set has a high dimension, quickly solving problems where the data have 10000 attributes with 1000000 observations on a personal computer [4].

Regarding the construction of the anomaly detector, three steps are required. The first is to calculate the sample set's left $(F_1(x),...,F_d(x))$ and right $(\overline{F_1}(x),...,\overline{F_d}(x))$ tail ECDFs, using equation (8). The asymmetry vector $b=[b_1,...,b_d]$ is also calculated in this first step, shown by equation (10) [4].

$$b_i=\frac{\frac{1}{n}\sum_{i=1}^{n}(x_i-\overline{x_i})^3}{\sqrt{\frac{1}{n-1}\sum_{i=1}^{n}(x_i-\overline{x_i})^2}^3}, \quad (10)$$

where *b* is the standard formulation for estimating asymmetry and *x* is the input data. The second step is calculating the copula's empirical observations for each input set, shown by equation (11) [4].

$$(U_{1,i},...,U_{d,i})=(F_1(X_{1,i}),...,F_d(X_{d,i})), \quad (11)$$

where *U* is the copula's empirical observations and X is the input data. With this calculation, we obtain the left tail and $V_{d,i}=\overline{F_d}(x_i)$, the right tail. Using the asymmetry equation to correct the empirical observations, we obtain $W_{d,i}=U_{d,i}$ if $b_d\leq 0$, and otherwise $W_{d,i}=V_{d,i}$ [4].

The third and final step is calculating the scores from the previous step, where the maximum negative logarithm of the probability generated by the empirical copula of the left, right, and asymmetry-corrected tails are outliers [4].

The Local Outlier Factor (LOF) algorithm was used to develop a semi-supervised model where only the restricted neighborhood of each object is considered. For most objects in a cluster, their LOF is approximately equal to 1, and for other objects, a lower and upper bound is applied, where these bounds emphasize their local nature. The LOF of the object is based on the number of neighbors closest to the neighborhood location of this object, where this number will be used to find possible local anomalies [1].

With the number of nearest neighbors defined, it is possible to calculate the accessibility distance, the maximum distance between two points, shown in equation (12).

$$reach\_dist_k(p,o)=\max\{kdist(o),d(p,o)\}, \quad (12)$$

where *k* is a natural number and *p* is an object related to object *o*. If the object *p* is within the neighborhood *k* of object *o*, then the reachability distance will be *k*.

Otherwise, it will be the distance between *p* and *o* [1]. Fig. 2 illustrates this step.

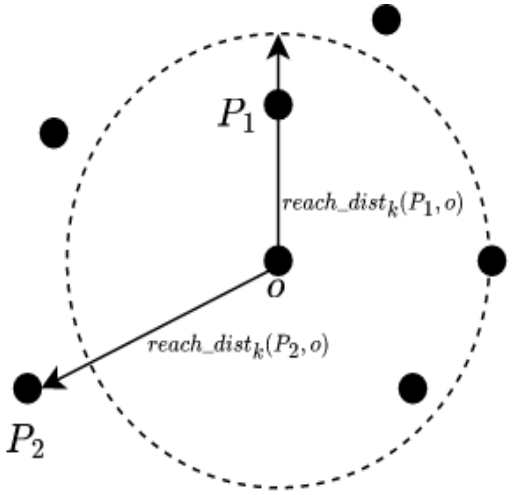


*Fig. 2: Reachability Density.*

Then the Local Reachability Density (LRD) is calculated. Here, two parameters are considered that define the density, the first is *MinPts*, which is the minimum number of objects, and the second is the volume. Equation (13) demonstrates this calculation, which uses the parameter *reach_dist* as a measure of importance [1].

$$LRD_{MinPts}(p) = \frac{1}{\frac{\sum o \in N_{MinPts}(p)(reach\_dist_{MinPts})}{|N_{MinPts}(p)|}}, \quad (13)$$

where LRD is the local reachability density and *p* is the object to be compared with the object *o*. Finally, the parameter calculated in equation (13) is compared with other neighbors, shown in equation (14) [1].

$$LOF_{MinPts}(p) = \frac{\sum o \in N_{MinPts}(p)(\frac{LRD_{MinPts}(o)}{LRD_{MinPts}(p)})}{|N_{MinPts}(p)|}, \quad (14)$$

The purpose of equation (14) is to evaluate possible novelties and test new elements in the set [1].

In two conditions, an aluminum beam 500 mm long, 38 mm wide, and 3.2 mm thick was used for the proposed experiment. The first, without any damage, is called the baseline, and the second, on one of the faces of the beam, a superficial machining with 30 mm of width was made to simulate damages. The experiments were conducted at the LMEst (Structural Mechanics Laboratory) at FEMEC-UFU. Fig. 3 demonstrates this step.

*Fig. 3: surface machining.*

At 70 mm on the opposite side of where the machining took place, a PZT patch of 1 mm thick and 20 mm in diameter was coupled to 100 mm from the edge of the structure to measure the impedance data of the specimen in the two conditions already mentioned, shown in Fig. 4.

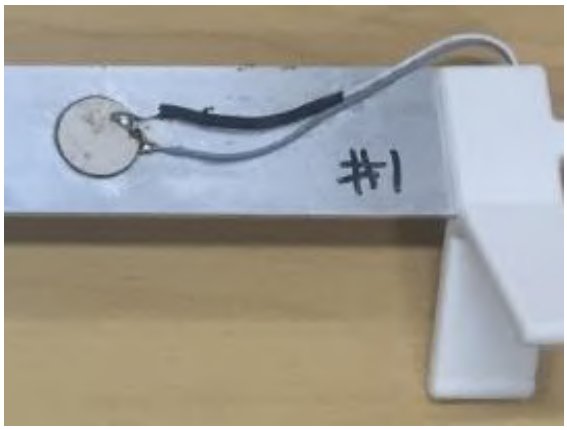


*Fig. 4: PZT patch coupled to the beam*

As shown in Fig. 3 and Fig. 4, two supports were built for the beam using a 3d printer and inserted on each side so that the specimen is adequately positioned and does not suffer interference from the base. Finally, the whole set can be seen in Fig. 5.

*Fig. 5: Beam used in the analysis*

For real-world problems, one of the main impact factors on computational resolutions is temperature, which in this experiment is the primary source of noise in the technique since thermal variation can induce structural

deformations and cause changes in the mechanical behavior of the piezoelectric material. Due to this, to simulate variations of this external factor, the aluminum beam was inserted in an EPL-4H climatic chamber of the Platinous series so that the data collection is more similar to real problems in different daily lives, as shown in Fig. 6.

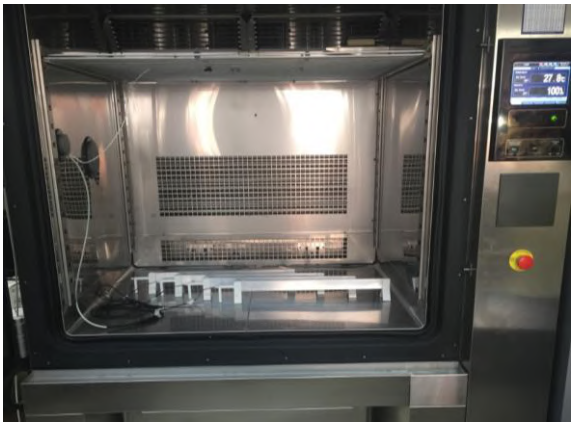

*Fig. 6: EPL-4H temperature chamber.*

Three temperature levels were chosen in the chamber, ranging from 13◦C to 22◦C, rising every 3◦C. After the impedance data collection was complete, the chamber increased the temperature and kept for 30 minutes. Later, stabilization and data collection occurred again. Thus, with three temperature sets, two baseline levels, seven damage levels, and 30 repetitions, 810 impedance signatures were collected. Therefore, there were 180 baselines and 630 damaged signatures in this study. These data were collected by an acquisition board connected to the PZT patch and stored on a server close to the chamber.

## III. RESULTS AND DISCUSSIONS

With the data collected and grouped in a spreadsheet file, it was possible to apply the algorithms (COPOD, LOF, and logistic regression) with the libraries, as follows, in the Python language, shown in Table 1.

*Table. 1: Libraries in Python*

| Model | Library |
|---|---|
| **Logistic Regression** | Scikit-learn |
| **COPOD** | Pyod |
| **LOF** | Scikit-learn |

Starting with the supervised Logistic Regression algorithm, 125 impedance signatures from baseline 1 and 154 signatures corresponding to damage levels 2 to 7 were used for training since the training of this model must occur with both classes, and the data should preferably be balanced. To test the classifier, 55 samples equivalent to baselines and 476 samples comparable to damages were used. It is essential to say that samples were chosen randomly.

For training the COPOD unsupervised algorithm, 180 samples from baselines were used with a contamination level of 0.25 to make the detector more judicious. For testing, 630 samples corresponding to all damage levels were used. Since this method is unsupervised, there is no need to split samples in training and test groups.

For the training of the LOF algorithm in a semi-supervised way, 125 baselines and 88 damaged samples were used for training. Two other vital parameters are the number of neighbors, defined as 15, and the contamination level, defined as 0.5, with the same objective mentioned before. Table 2 shows the results of each model.

*Table. 2: Experimental Results*

| Model | Total Amount of Samples | Anomalies Identified |
|---|---|---|
| **Logistic Regression** | 531 | 100% |
| **COPOD** | 810 | 88.7% |
| **LOF** | 597 | 95.7% |

As can be seen from Table 2, all anomaly identifiers techniques could be applied for failure prediction since they are actual data obtained experimentally from structures.

Figures 7-9 are shown below, describing the confusion matrices for each model.

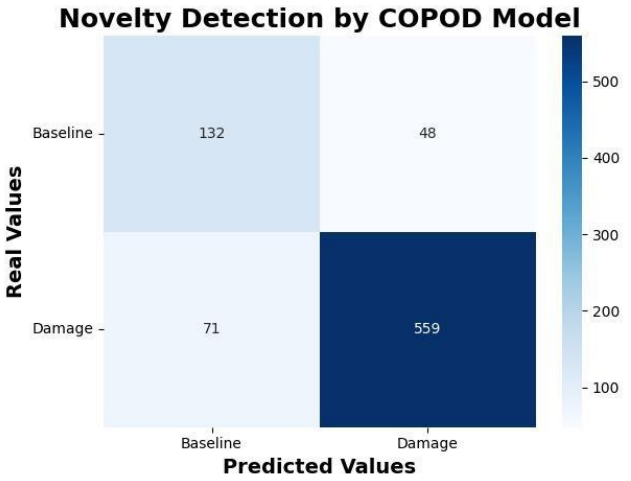


*Fig. 7: Confusion Matrix - COPOD*

According to Fig. 7, the COPOD model identified 132 baseline cases correctly, while it was wrong (type I) in 48 cases. However, in the most critical case, the correct detection of damage (anomaly), the algorithm found 559 signatures correctly, missing 71 signatures (type II). This second type of error is more harmful, as 71 damage conditions were analyzed as a baseline.

The semi-supervised LOF algorithm obtained a better result than COPOD, as shown in Fig. 8.

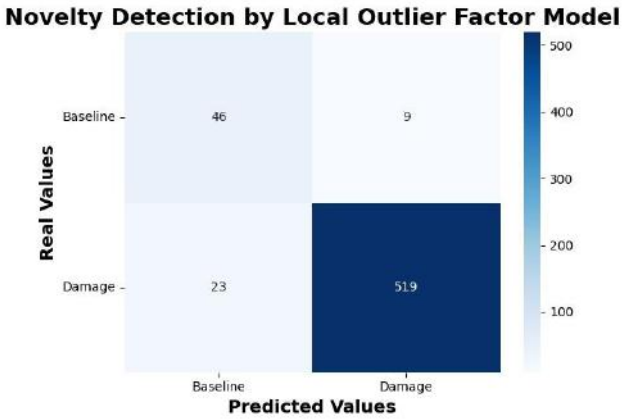


*Fig. 8: Confusion Matrix - LOF*

In this second method, type I and II errors were more minor, and the severe cases of false negatives were only 23 concerning 519 true positives.

Figure 9 shows the confusion matrix of the model based on Logistic Regression.

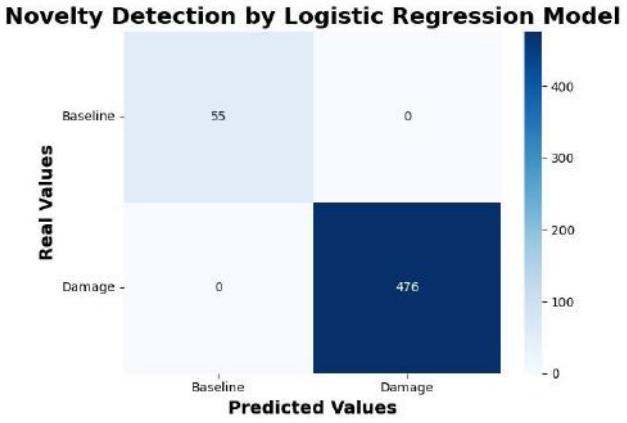


*Fig. 9: Confusion Matrix – Logistic Regression*

Finally, the model with the best result obtained, perhaps as expected, is the supervised model in which there were no occurrences of both types I and II errors.

## IV. CONCLUSION

This contribution compared anomaly detection models based on three types of machine learning: supervised, unsupervised and semi-supervised, and Logistic Regression, COPOD, and LOF. After making a theoretical reference to impedance-based structural integrity monitoring (ISHM) as well as machine learning techniques, the problem to be solved was exposed. This issue consists of the possibility of identifying anomalies concerning a specimen with damage conducted on one of the faces. This object was moved to a climatic chamber to simulate temperature variations.

Logistic Regression and LOF algorithms correctly identified all levels of anomalies. In the first model, due to the training occurring together with the label, it was possible to detect all the impedance signature points concerning the inferred damages in the beam through superficial machining. In the second model, semi-supervised learning is also known as novelty detection; in training, all data are considered baseline. After this step, the detector correctly identified all data's novelty about anomalies.

The COPOD algorithm was the worst at detecting anomalies, with 88.7% accuracy. This result could be expected because it is an unsupervised technique and does not provide information for model training. However, in an actual structural monitoring condition, this level of accuracy can be significant and applied in monitoring systems with redundancy.

The second result obtained through the semi-supervised LOF technique can be considered an excellent potential for actual application due to its 95.7% accuracy in damage detection.

The best result, with 100% accuracy, was the supervised model based on Logistic Regression. However, in monitoring real structures, the training process is only sometimes possible, considering that the structure already starts in a lifetime behavior in use. Finally, all methods presented excellent application possibilities in fault detection, in addition to being relatively simple techniques to be implemented, including in microcontrollers, allowing the development of intelligent sensors for fault prediction.

## REFERENCES

[1] BREUNIG, M. M. et al. Lof: identifying density-based local outliers. In: Proceedings of the 2000 ACM SIGMOD international conference on Management of data. [S.l.: s.n.], 2000. p. 93–104.

[2] GÉRON, A. Mãos à Obra: Aprendizado de Máquina com Scikit-Learn & TensorFlow. [S.l.]: Alta Books, 2019.

[3] GIURGIUTIU, V.; ZAGRAI, A. Damage detection in thin plates and aerospace structures with the electro-mechanical impedance method. Structural Health Monitoring, Sage Publications Sage CA: Thousand Oaks, CA, v. 4, n. 2, p. 99–118, 2005.

[4] LI, Z. et al. Copod: copula-based outlier detection. In: IEEE. 2020 IEEE International Conference on Data Mining (ICDM). [S.l.], 2020. p. 1118–1123.

[5] LIANG, C.; SUN, F. P.; ROGERS, C. A. Coupled electro-mechanical analysis of adaptive material systems-determination of the actuator power consumption and system energy transfer. Journal of intelligent material systems and structures, TECHNOMIC PUBLISHING CO., INC. 851 New Holland Ave., Box 3535, Lancaster, PA ..., v. 8, n. 4, p. 335–343, 1994.

[6] MINUSSI, J. A.; DAMACENA, C.; JR, W. L. N. Um modelo de previsão de solvência utilizando regressão logística. Revista de Administração Contemporânea, SciELO Brasil, v. 6, n. 3, p. 109–128, 2002.

[7] MUGANDA, J. M. et al. Influence function measurement technique using the direct and indirect piezoelectric effect for surface shape control in adaptive systems. IEEE Transactions on Automation Science and Engineering, v. 19, n. 2, 2022.

[8] NEPOMUCENO, L. X. Técnicas de manutenção preditiva-vol. 1. [S.l.]: Editora Blucher, 2014. v. 1.

[9] NETO, J. C. da S.; LIMA, A. Gonçalves de. Implantação do controle de manutenção. Revista Club de Mantenimiento, n. 10, 2002.

[10] REZENDE, S. W. F. de; BARELLA, B. P.; JR, J. d. R. V. M. Damage identification of vehicle brake disks by the use of impedance-based shm and unsupervised machine learning method. INTERNATIONAL JOURNAL OF ADVANCED ENGINEERING RESEARCH AND SCIENCE, v. 7, p. 324-330, 2020a, 2020.

[11] REZENDE, S. W. F. de et al. Convolutional neural network and impedance-based shm applied to damage detection. Engineering Research Express, IOP Publishing, v. 2, n. 3, p. 035031, 2020.